

Band structure analysis of the conduction-band mass anisotropy in 6H and 4H SiC

Walter R. L. Lambrecht and Benjamin Segall
*Department of Physics, Case Western Reserve University
 Cleveland, OH-44106-7079*
 (February 8, 2008)

The band structures of 6H SiC and 4H SiC calculated by means of the full-potential linear-muffin-tin orbital method are used to determine the effective mass tensors for their conduction-band minima. The results are shown to be consistent with recent optically detected cyclotron resonance measurements which find the ratio of cyclotron masses for $\mathbf{B} \perp \mathbf{c}$ to $\mathbf{B} \parallel \mathbf{c}$ to be larger (smaller) than unity for the 6H (4H) polytype. However, contrary to previous suggestions, appreciable anisotropies in the c -plane are found. For 6H SiC, a strong dependency on band-filling is predicted because of the occurrence of a double well minimum along the ML -axis. The calculated mass tensors for 3C and 2H are also reported.

PACS numbers: 71.25.Jd 71.25.Tn

The technological potential of SiC for high-temperature, high-power and high-frequency electronic devices as well as the intrinsic scientific interest of the polytypism of SiC have been recognized for several decades. Only recently, however, has it become possible to obtain electronic grade quality single crystal single polytype material. Recently, it was found that 4H SiC exhibits a much smaller (and opposite) anisotropy of the electron mobility with respect to the c -axis than does 6H SiC.^{1,2} It has been unclear up to now whether this could be attributed to a corresponding anisotropy in the effective mass tensors. Rather conflicting results have been reported on the effective masses as determined by a fitting of IR absorption spectra of the excited shallow donor states^{3,4} and by optically detected cyclotron resonance (ODCR).^{5,6}

In this letter, calculated band structures of 6H SiC and 4H SiC are used to determine the effective mass tensors at the conduction-band minimum. Our results are in good agreement with the ODCR results on the anisotropies with respect to the c -axis for 6H and 4H SiC masses and hence support a mass-anisotropy as the cause for the mobility anisotropies. Our calculations also predict appreciable anisotropies of the mass tensors in the c -plane. In addition, they predict a strong dependency of the masses on band-filling in the case of 6H SiC due to a double-well-like conduction-band minimum.

Our band-structure calculations were performed within the density functional theory in the local density approximation (LDA)⁷ using the full-potential (FP) linear muffin-tin orbital method.^{8,9} They differ in some small, but for the present purpose relevant details, from our earlier results¹⁰ which used the atomic sphere approximation (ASA).¹¹ The previous calculations were already found to provide a satisfactory account of the UV-

reflectivity spectra.¹² In the present work, we performed calculations on a fine mesh of \mathbf{k} -points in order to examine the details of the energy-band surfaces close to the conduction-band minima.

In 6H SiC, the minimum is found about halfway between M and L along the $ML \equiv U$ -axis of the 6H-Brillouin zone.¹³ This leads to a 6-valley model in which the valleys occur in 3 pairs with each pair being separated by a small barrier (of 9.5 meV) at the three equivalent M points. The lowest band along this line can be well approximated by a fourth order polynomial in $|k_z|$, with z chosen along \mathbf{c} . In the directions parallel to $M\Gamma$ (or $[10\bar{1}0]$) and MK (or $[2\bar{1}\bar{1}0]$), respectively called the x - and y -directions, the bands are found to behave parabolically near the minimum with the masses there almost equal to those at M . The cyclotron masses for orbits not in the c -plane are calculated from $m = (\hbar^2/2\pi)\partial A/\partial E$, with A the cross-sectional area of the extremal orbit on the constant energy surface calculated numerically from the fitted energy bands. By varying the energy E of the chosen constant energy surface, we obtain the variation of the mass with conduction band filling.

In 4H SiC the minimum is found¹⁴ at M and the bands are parabolic in the three symmetry directions of the crystal up to at least 300 meV above the minimum. In fact, there are two bands at M within less than 100 meV of each other whose energetic position was found to be sensitive to the details of the calculation. Specifically, these bands were interchanged in the ASA calculation. Apart from this interchange, the results from FP and ASA calculations were in very good agreement (including the masses of each of these bands).

The first three rows in Table I give the principal components of the mass tensor at the ML minimum in 6H SiC and at the M minima in 4H and 2H SiC. Clearly, these are fully anisotropic (i.e. $m_1 \neq m_2 \neq m_3$ with 1, 2, 3 corresponding to x, y, z .) This is consistent with the C_{2v} symmetry for points on the ML axis. 2H SiC is included although its lowest conduction band minimum is at K (in the equatorial plane at the corner of the hexagon.) It can be seen that the 2H masses at M are more similar to those of 6H than those of 4H. Similar closer similarity between 6H and 2H than between 4H and 2H was previously also found in other aspects of the band structure.¹² The mass tensor at K is rotationally invariant about the c -axis as required by the C_{3v} symmetry of the K -point and has the values: $m \parallel c = 0.27$ and $m \perp c = 0.45$.

The cyclotron effective mass associated with a single

ellipsoid is:

$$m^* = \sqrt{\frac{m_1 m_2 m_3}{m_1 b_1^2 + m_2 b_2^2 + m_3 b_3^2}}, \quad (1)$$

where b_i are the direction cosines of \mathbf{B} with the principal axes of the mass tensor. To compare our results with the ODCR measurements it is necessary to consider the combined effect of the different valleys which for a general orientation of the magnetic field \mathbf{B} become inequivalent. For \mathbf{B} along the c-axis, the 3 valleys for 4H (or double valleys for 6H) at the different M -points are equivalently oriented; consequently only one peak is observed in ODCR with an effective mass $m_{\perp}^* = \sqrt{m_1 m_2}$. Our values for this effective mass are given in the sixth row of Table I and are in good agreement with the ODCR values of 0.42 ± 0.02 in both 4H and 6H SiC. The slight underestimate of the calculated masses for 4H is partially due to the absence of phonon renormalization contributions and may also partially be due to the LDA. In this connection we note a similar situation in 3C-SiC. There, our calculated values for the electron mass are $m_l = 0.63$, $m_t = 0.23$, while the values measured by cyclotron resonance¹⁶ are $m_l = 0.677$ and $m_t = 0.247$. (Here *longitudinal* (l) and *transverse* (t) refer to the directions parallel and perpendicular to the cubic $\Gamma - X$ axis for the X -minimum.)

For \mathbf{B} in the c-plane, the ellipsoids at the various M or ML points are generally oriented differently with respect to the field and should give rise to three peaks in ODCR. For the [10̄10] and [21̄10] directions, two of the peaks coincide. The variation of the masses in the c-plane is shown in Fig. 1 as a function of azimuthal angle ϕ measured from the [10̄10] direction.

The published ODCR measurements using microwave frequencies of 9.235 GHz in the X-band do not report anisotropy in the c-plane and were analysed as if the valleys were ellipsoids of revolution with a m_{\perp} and m_{\parallel} , where \perp and \parallel refer to the c-axis. Fig. 2 shows simulated ODCR microwave absorption spectra based on the calculated masses for 4H SiC and 6H SiC for a number of important directions. The $\omega\tau$ values (microwave frequency times lifetime) used are close to those deduced from the experiments of Son *et al.*^{5,6}. Because of the width of the ODCR signals from the differently oriented ellipsoids, the in-plane sum peak is seen to show little variation in position. This explains why the ODCR spectra appear to give an isotropic in-plane mass in spite of the fact that each ellipsoid is strongly anisotropic in the plane. When the effective in-plane masses are equated to $\sqrt{m_{\perp}^* m_{\parallel}^*}$, as is appropriate for a model with in-plane rotationally invariant ellipsoids, the effective m_{\parallel}^* 's in Table I are obtained.

Son *et al.*⁵ also reported an ODCR signal using a higher microwave frequency in the Q-band ($\nu = 35$ GHz). With the correspondingly higher $\omega\tau = 9.1$ value, our calculations predict that the mass anisotropy in the c-plane should be clearly resolved for 4H, as can be seen in Fig. 3. Very recently, such in-plane anisotropy was confirmed by

Hofmann *et al.*¹⁷. The mass values deduced from these new experiments ($m_1 = 0.58$, $m_2 = 0.31$ and $m_3 = 0.33$) are in good agreement with our calculated values.

For 6H SiC, the strong non-parabolicity resulting from the double well character of the minima along the ML axis leads to a variation of the masses with energy above the minimum ($E - E_c$) (or, band filling). Fig. 4 shows the variation with $E - E_c$ of $\sqrt{m_1 m_3}$, $\sqrt{m_2 m_3}$ and the effective m_{\parallel}^* deduced from the calculated broad peak in microwave absorption for $\mathbf{B} \perp \mathbf{c}$ in the manner explained above. The calculated m_{\parallel}^* is seen to gradually increase with band filling up to the barrier, at which point there is a discontinuity because the orbits then encircle the double minimum centered at M instead of the separate valleys. At higher energies m_{\parallel}^* decreases with increasing energy. In the degenerate limit, a Fermi energy just at the barrier corresponds to a carrier concentration of the order of 10^{19} cm^{-3} . While carrier concentrations of this magnitude are certainly possible, the carrier concentrations in the ODCR measurements⁶ (at 6K) which are produced by optical pumping are expected to be much lower. Based on the laser intensity employed and the carrier lifetimes¹⁸ we estimate concentrations of the order of 10^{15} cm^{-3} . On the other hand, the high microwave powers used (> 20 mW) may lead to a non-equilibrium hot carrier distribution and hence the experiment may conceivably probe masses higher in the band.

As can be seen in Table I, the two calculated 4H masses and m_{\perp}^* for 6H SiC are in excellent agreement with experiment. Also consistent with experiment, m_{\parallel}^* in 6H SiC is relatively large. Nevertheless, this mass is 40 % smaller than experiment. Several factors, including the non-parabolicity noted above could bear on this discrepancy. The polaron renormalization mass increase could be substantial for this large mass because the polaron coupling constant increases with mass. Electron-electron interaction corrections to the LDA may also alter the masses, but are unlikely to be significant in view of the good agreement for the other masses. Finally, we note that the experimental uncertainty on this mass is fairly large because it depends on fitting a broad resonance. Considering the above factors, the agreement between the calculated and measured values for 6H m_{\parallel}^* may be called fair.

In conclusion, the agreement between our calculated effective mass tensors and ODCR measurements is excellent for 4H SiC and semiquantitative for 6H SiC. Although we found the effective mass tensors to be fully anisotropic in both polytypes, we explain why the recent X-band ODCR measurements did not resolve the superposition of the fairly broad resonant peaks for $\mathbf{B} \perp \mathbf{c}$. That lead to the erroneous suggestion that the in-plane mass is isotropic. In agreement with the ODCR studies, we find the ratio $m_{\parallel}^*/m_{\perp}^* < 1$ for 4H and > 1 for 6H SiC. The in-plane anisotropy is predicted by our calculations to be observable with higher $\omega\tau$ values as was confirmed very recently for 4H SiC by ODCR measure-

ments using a higher microwave frequency.¹⁷ We further predict a considerable dependence of m_{\parallel}^* in 6H SiC on band filling due to the double well character of the lowest conduction band. This could influence transport properties and may also be detectable in future ODCR measurements with higher band fillings. The manner in which the effective masses enter the mobility anisotropy is far from trivial because the different scattering processes that could come in have different functional dependence on the masses. Nevertheless, whatever scattering mechanisms are involved, the mobility is expected to decrease when the mass increases. The calculated c-axis anisotropies of the mass tensor thus appear to be the basis of the observed large Hall mobility anisotropies in 6H and small and reversed one in 4H. However, further detailed work involving the effects of different scattering mechanisms will be required to quantitatively explain their magnitude and temperature dependence. Finally, it is clear that these rather unusual conduction-band minima call for an extension of effective mass theory before one can confidently deduce effective masses from donor excitation IR spectra.

We thank Drs. W. J. Choyke, R. P. Devaty, N. T. Son, D. M. Hofmann, D. Volm, and B. K. Meyer for stimulating discussions and for communicating unpublished results. This work was supported by the National Science Foundation, Grant No. DMR-92-22387 and Wright Laboratories through contract No. F33615-93-C-5347.

set was used on Si and C nearly touching muffin-tin spheres and additional s-orbitals were used on some of the empty spheres in the case of 6H SiC. Augmentation and fitting cut-offs were $l_{max} = 4$ on atoms and $l_{max} = 2$ on empty spheres. 12 special k-points were used in the Brillouin-zone integrations. Complete details and results of these calculations, which were found to be adequately converged with respect to all relevant parameters, will be presented elsewhere.

- ¹⁰ W. R. L. Lambrecht in *Diamond, SiC and Nitride Wide Bandgap Semiconductors*, edited by C. H. Carter, Jr., G. Gildenblat, S. Nakamura, and R. J. Nemanich, Mater. Res. Soc. Symp. Proc. Vol. 339, p. 565 (1994).
- ¹¹ O. K. Andersen, O. Jepsen, and M. Šob, in *Electronic Band Structure and its Applications*, edited by M. Yussouff, (Springer, Heidelberg, 1987) p. 1.
- ¹² W. R. L. Lambrecht, B. Segall, M. Yoganathan, W. Sutrop, R. P. Devaty, W. J. Choyke, J. A. Edmond, J. A. Powell, and M. Alouani, *Phys. Rev. B* **50**, 10722 (1994).
- ¹³ The M point lies in the equatorial plane ($k_z = 0$) at the midpoint of the hexagon sides, while L lies above it in the top plane ($k_z = \pi/c$); see e.g. C. J. Bradley and A. P. Cracknell, *The Mathematical Theory of Symmetry in Solids: Representation Theory for Point Groups and Space Groups*, (Clarendon Press, Oxford 1972).
- ¹⁴ The location of the minimum at M in 4H SiC has been under debate because of the claim by L. Patrick, W. J. Choyke, and D. R. Hamilton, *Phys. Rev.* **137**, A1515 (1965) that phonon-replica in luminescence spectra indicate that the minima occur at lower symmetry F -points. We will show elsewhere that the spectrum is in fact consistent with a M -minimum. This demonstration utilizes the recent phonon calculations by M. Hofmann, A. Zywiertz, K. Karch, and F. Bechstedt, *Phys. Rev. B* **50**, 13401 (1994). In addition, the present results for the masses indirectly confirm the location of the minimum at M .
- ¹⁵ L. Patrick, *Phys. Rev. B* **5**, 2198 (1972).
- ¹⁶ R. Kaplan, R. J. Wagner, H. J. Kim, and R. J. Davis, *Solid State Commun.* **55**, 67 (1985).
- ¹⁷ D. M. Hofmann, D. Volm, and B. K. Meyer, private communication.
- ¹⁸ N. T. Son, private communication.

¹ W. J. Schaffer, G. H. Negley, K. G. Irvine, and J. W. Palomar, in *Diamond, SiC and Nitride Wide Bandgap Semiconductors*, edited by C. H. Carter, Jr., G. Gildenblat, S. Nakamura, and R. J. Nemanich, Mater. Res. Soc. Symp. Proc. Vol. 339, p. 595 (1994).

² M. Schadt, G. Pensl, R. P. Devaty, W. J. Choyke, R. Stein, and D. Stephani, *Appl. Phys. Lett.* **65**, 3120 (1994).

³ W. Sutrop, G. Pensl, W. J. Choyke, R. Stein, and S. Leibenzeder, *J. Appl. Phys.* **73**, 3708 (1992)

⁴ W. Götz, A. Schöner, G. Pensl, W. Sutrop, W. J. Choyke, R. Stein, and S. Leibenzeder, *J. Appl. Phys.* **73**, 3332 (1993)

⁵ N. T. Son, W. M. Chen, O. Kordina, A. O. Konstantinov, B. Monemar, E. Janzén, D. M. Hofmann, D. Volm, M. Drechsler, and B. K. Meyer, *Appl. Phys. Lett.* **66**, 1074 (1995).

⁶ N. T. Son, O. Kordina, A. O. Konstantinov, W. M. Chen, E. Sörman, B. Monemar, and E. Janzén, *Appl. Phys. Lett.* **65**, 3209 (1994).

⁷ P. Hohenberg and W. Kohn, *Phys. Rev.* **136**, B864 (1964); W. Kohn and L. J. Sham, *Phys. Rev.* **140**, A1133 (1965); L. Hedin and B. I. Lundqvist, *J. Phys. C* **4**, 2064 (1971).

⁸ M. Methfessel, *Phys. Rev. B* **38**, 1537 (1988).

⁹ The calculations were performed at the experimental a lattice constant using an ideal c/a ratio. A triple κ dds basis

TABLE I. Principal components of the conduction-band effective mass tensor (in units of the free electron mass) for 6H (ML -minimum), 4H and 2H SiC (at M -minimum) and derived quantities.

		6H	4H	2H
m_1	$M\Gamma$	0.77	0.58	0.95
m_2	MK	0.24	0.28	0.15
m_3	ML	1.42	0.31	1.07
$m_{xz} = \sqrt{m_1 m_3}$	$\Gamma - M - L$	1.05	0.42	1.01
$m_{yz} = \sqrt{m_2 m_3}$	$K - M - L$	0.59	0.29	0.40
$m_{xy} = \sqrt{m_1 m_2}$	$\Gamma - M - K$	0.43	0.40	0.38
$m_{\perp}^* = \sqrt{m_1 m_2}$ (expt.) ^a	$\mathbf{B} \parallel \mathbf{c}$	0.42	0.42	
$\sqrt{m_{\perp}^* m_{\parallel}^*}$ (expt.) ^a	$\mathbf{B} \perp \mathbf{c}$	0.92	0.35	
$\sqrt{m_{\perp}^* m_{\parallel}^*}$ (theory)		0.67-0.89 ^b	0.33	
m_{\parallel}^* (expt.) ^a		2.0±0.2	0.29	
m_{\parallel}^* (theory)		1.1-2.0 ^b	0.27	
$m_{\parallel}^*/m_{\perp}^*$ (expt.) ^a		4.8	0.69	
$m_{\parallel}^*/m_{\perp}^*$ (theory)		2.5-4.6 ^b	0.68	

^aSon et al.^{5,6}

^bDepending on band filling: first value near bottom of the band, second near barrier crossing

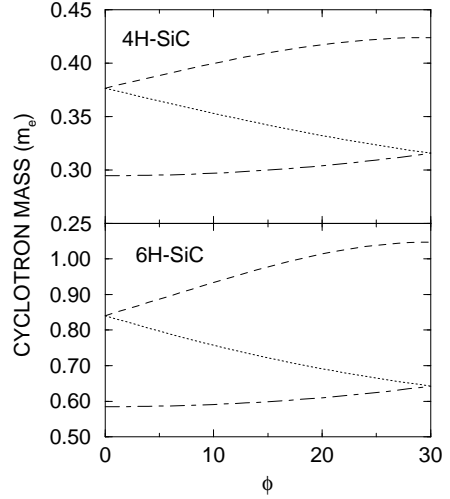


FIG. 1. Cyclotron masses in c-plane for 6H and 4H SiC as function of azimuthal angle ϕ . $\phi = 0$ corresponds to $[10\bar{1}0]$ and $\phi = 30^\circ$ to $[2\bar{1}\bar{1}0]$. The line type corresponds to the individual contributions to the ODCR spectra shown in Fig. 3.

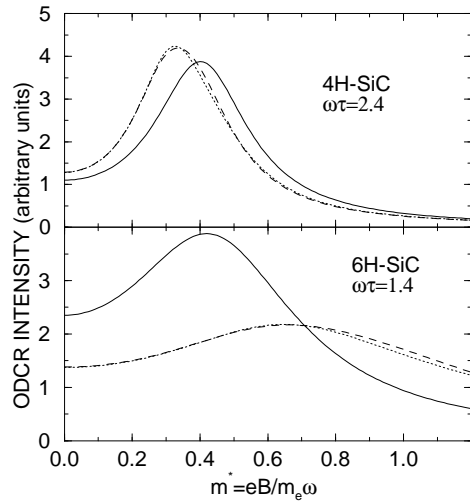


FIG. 2. Simulated X-band (9.235 GHz) ODCR spectra for 4H SiC and 6H SiC. Solid line, $\mathbf{B} \parallel [0001]$; dashed line, $\mathbf{B} \parallel [10\bar{1}0]$; dotted line, $\mathbf{B} \parallel [2\bar{1}\bar{1}0]$

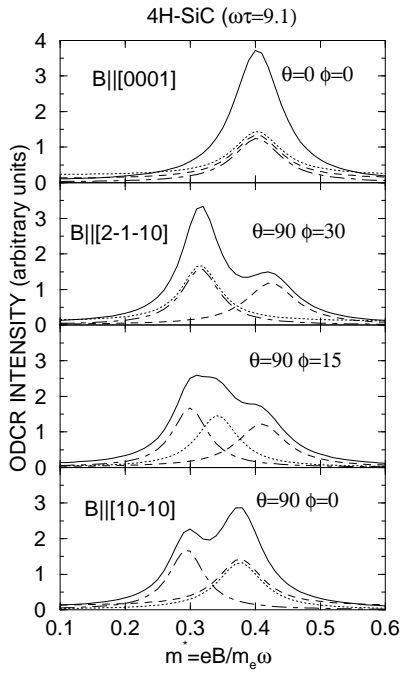


FIG. 3. Simulated Q-band (35 GHz) ODCR spectra for 4H SiC using $\omega\tau = 9.1$ for various orientations of the magnetic field. The dashed, dotted and dot-dashed lines correspond to the individual effective mass contributions shown in Fig. 1 and the solid lines to their sums. For clarity, slight off-sets are included where two identical peaks overlap.

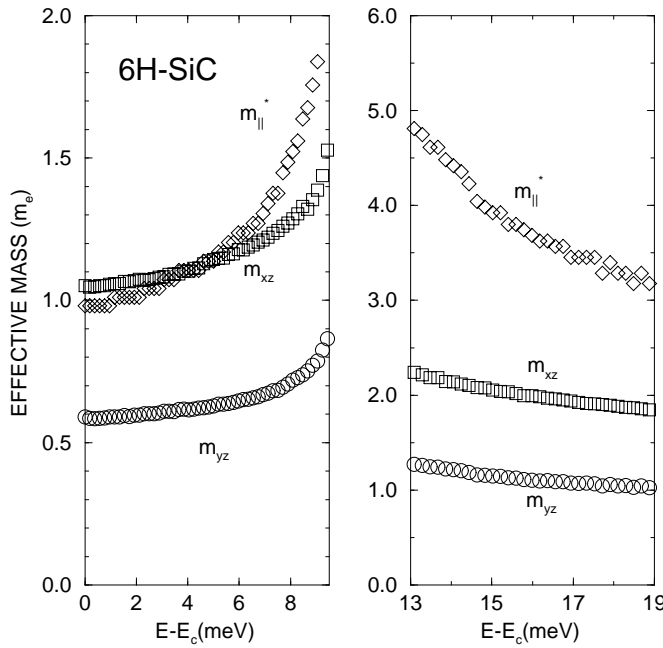


FIG. 4. Calculated effective masses in 6H SiC as a function of conduction band filling. The six-valley region below the barrier is shown separately from the three-valley region above. m_{xz} and m_{yz} are defined in Table I. m_{\parallel}^* is a pseudo-effective mass parallel to c appearing in the isotropic in-plane model discussed in the text.